

1-1-2012

## A surface based approach for cortical thickness comparison between PiB+ and PiB-healthy control subjects

V Dore

P Bourgeat

J Fripp

O Acosta

G Chetelat

*See next page for additional authors*

Follow this and additional works at: <https://ro.ecu.edu.au/ecuworks2012>



Part of the [Medicine and Health Sciences Commons](#)

---

10.1117/12.911752

This is an Author's Accepted Manuscript of: Dore, V., Bourgeat, P., Fripp, J., Acosta, O., Chetelat, G., Szoeki, C., Ellis, K., Martins, R. N., Villemagne, V., Masters, C., Ames, D., Rowe, C., & Salvado, O. (2012). A surface based approach for cortical thickness comparison between PiB+ and PiB-healthy control subjects. Proceedings of Medical Imaging 2012: Image Processing. (pp. 831413-1to 831413-6). San Diego, California. SPIE. Available [here](#)

This Conference Proceeding is posted at Research Online.

<https://ro.ecu.edu.au/ecuworks2012/204>

---

**Authors**

V Dore, P Bourgeat, J Fripp, O Acosta, G Chetelat, C Szoeki, Kathryn Ellis, Ralph Martins, V Villemagne, C L Masters, D Ames, C O Rowe, and O Salvado

Vincent Doré ; Pierrick Bourgeat ; Jurgen Fripp ; Oscar Acosta ; Gael Chetelat ; Cassandra Szoeki ; Kathryn A. Ellis ; Ralph N. Martins ; Victor Villemagne ; Colin L. Masters ; David Ames ; Christopher C. Rowe ; Olivier Salvado; "A surface based approach for cortical thickness comparison between PiB+ and PiB- healthy control subjects". Proc. SPIE 8314, Medical Imaging 2012: Image Processing, 831413 (February 23, 2012); doi:10.1117/12.911752.

Copyright 2012 Society of Photo-Optical Instrumentation Engineers. One print or electronic copy may be made for personal use only. Systematic reproduction and distribution, duplication of any material in this paper for a fee or for commercial purposes, or modification of the content of the paper are prohibited.

<http://dx.doi.org/10.1117/12.911752>

## A Surface Based approach for cortical thickness comparison between PiB+ and PiB- Healthy Control subjects

Vincent Doré<sup>a</sup>, Pierrick Bourgeat<sup>a</sup>, Jurgen Fripp<sup>a</sup>, Oscar Acosta<sup>b</sup>, Gael Chetelat<sup>d</sup>, Cassandra Szoeké<sup>e</sup>, Kathryn A. Ellis<sup>f,g,h</sup>, Ralph N. Martins<sup>i,j</sup>, Victor Villemagne<sup>c</sup>, Colin L. Masters<sup>g,k</sup>, David Ames<sup>f,h</sup>, Christopher C. Rowe<sup>c</sup>, Olivier Salvado<sup>a</sup> and the AIBL Research Group

<sup>a</sup> Australian e-Health Research Centre, ICT Centre, CSIRO, Herston, Australia;

<sup>b</sup> INSERM, Rennes, France and Université de Rennes 1, LTSI, France

<sup>c</sup> Department of Nuclear Medicine and Centre for PET, and Department of Medicine, University of Melbourne, Austin Hospital, Melbourne, VIC, Australia

<sup>d</sup> Inserm-EPHE-Université de Caen/Basse-Normandie, Unité U923, GIP Cyceron, CHU Côte de Nacre, Caen, France

<sup>e</sup> CSIRO, Parkville, Victoria, Australia

<sup>f</sup> Academic Unit for Psychiatry of Old Age, Department of Psychiatry, The University of Melbourne, St. Vincent's Aged Psychiatry Service, St George's Hospital, VIC Australia

<sup>g</sup> The Mental Health Research Institute, University of Melbourne, Parkville, VIC, Australia

<sup>h</sup> National Ageing Research Institute, Parkville, VIC, Australia

<sup>i</sup> Centre of Excellence for Alzheimer's Disease Research and Care, School of Exercise Biomedical and Health Sciences, Edith Cowan University, Joondalup, Western Australia, Australia

<sup>j</sup> Sir James McCusker Alzheimer's Disease Research Unit (Hollywood Private Hospital), Perth, Western Australia, Australia

<sup>k</sup> Centre for Neurosciences, University of Melbourne, Parkville, VIC, Australia

### ABSTRACT

$\beta$ -amyloid has been shown to play a crucial role in Alzheimer's disease (AD). In vivo  $\beta$ -amyloid imaging using [11C]Pittsburgh compound B (PiB) positron emission tomography has made it possible to analyze the relationship between  $\beta$ -amyloid deposition and different pathological markers involved in AD. PiB allows us to stratify the population between subjects which are likely to have prodromal AD, and those who don't. The comparison of the cortical thickness in these different groups is important to better understanding and detect the first symptoms of the disease which may lead to an earlier therapeutic care to reduce neurone loss.

Several techniques have been developed to compare the cortical volume and/or thickness between AD and HC groups. However due to the noise introduced by the cortical thickness estimation and by the registration, these methods do not allow to unveil any major different when comparing prodromal AD groups with healthy control subjects group. To improve our understanding of where initial Alzheimer neurodegeneration occurs in the cortex we have developed a surface based technique, and have applied it to the discrimination between PiB-positive and PiB-negative HCs. We first identify the regions where AD patients show high cortical atrophy by using an AD/PiB- HC vertex-wise T-test. In each of these discriminating regions, comparison between PiB+ HC, PiB- HC and AD are performed. We found some significant differences between the two HC groups in the hippocampus and in the temporal lobe for both hemisphere and in the precuneus and occipital regions only for the left hemisphere.

**Keywords:** MRI, PiB\_PET images, Surface based Approach, Statistical Population Analysis, Cortical thickness,  $\beta$ -amyloid, Alzheimer's disease

## 1. DESCRIPTION OF THE PURPOSE

The comparison of brain has proved to be a challenging task due to the convoluted geometry of the brain and the high inter-patient variability. A significant amount of research has focused on this problem; they can be divided into two main methods, the surface based [1] and the voxel based [2,3] approaches. Instead of handling complex 3D images, surface based methods extract a 3D mesh representing the outer layer of the cortex, which provides a more natural representation of surfacic nature of the cortex, and gives a more natural way to visualise the cortex in 3D. The surface-based approach starts with generating individual cortical surfaces from 3D brain images, mapping these surfaces to a template before performing inter-individual statistical analysis on each point of the template surface. However the noise introduced during the cortical thickness estimation and the registration doesn't allow surface based approaches unveiling any major cortical thickness difference when comparing groups with low difference.

In this paper, we propose a new surface based approach that makes it possible to compare HC having a low PiB (PiB SURV<1.5) retention with HC presenting a high PiB retention (PiB SURV>1.5). We first present a new surface based pipeline that propagates the local cortical thickness of each patient on a common template. A per-vertex T-test between PiB- HC and AD highlights regions where AD patient exhibit major cortical atrophy. Our hypothesis being that PiB+ HC will convert to AD, we only compare PiB+ with PiB- HC groups in these discriminating regions. Hence, the mean values of the cortical thickness are computed for each patient and in each discriminating regions and are then statistically compared. The use of discriminating regions enables to group vertexes that may exhibit cortical atrophy while computing the mean values enables to reduce the influence of noise and to increase the statistic. This approach can find significant differences between the two HC groups in the hippocampus and in the temporal lobe for both hemisphere and in the precuneus and occipital regions only for the left hemisphere.

## 2. METHOD

### 2.1 Cortical thickness estimation and Surface-based approach

119 subjects underwent a MRI scan on a 3T Siemens Trio using a 3D MPRAGE sequence and a 11C-PIB PET scans using a Philips ADAC Allegro full-ring tomograph as part of the Australian Imaging, Biomarker and Lifestyle study [4]. PiB scans were normalised with the standardized uptake value ratio (SUVR) method [5]. In the subject cohort, 29 patients were Alzheimer's disease, while the other 90 were healthy controls elderly subjects. 33 PiB+ HC had a neocortical PiB above 1.5 and were classified as PiB+ [6], while the remainder 57 subjects were classified as PiB-.

In a first stage, the MRI images are classified into three brain tissues (gray matter (GM), white matter (WM) and CSF) with an expectation maximization segmentation algorithm allowing the use of nine atlas [6]. For each MRI, the algorithm is initialized with the nine atlases. This approach allows reducing the mis-segmentation. The final segmentation is a consensus of the nine different segmentations provided by a voting process. At the same stage of the pipeline, the AAL and IBSR segmentations [7] of the atlas are propagated to each MRI in the cohort through a same voting process.

On the pure GM segmentation, topological constraints force the interface to be a continuous layer [8] over the WM. From the segmentation, a maximum a posteriori classification of voxel into pure and mixed tissues is performed along the GM/WM and GM/CSF boundaries, resulting in partial-volume coefficients of the GM (GMPVC) at each voxel. This latter coefficient is used in the next stage as a Laplacian initialization of the thickness estimation. An Eulerian PDEs approach is used for this purpose [9]. The cortical thickness is then mapped on the WM/GM interface. 3D meshes of the WM/GM interfaces are generated with a marching cube algorithm.

Segmentation and meshing errors result into tunnels and handles of the meshes. Tagglut [10] corrects the mesh topology to generate a genus zero mesh. In the first part of the algorithm the shortest non-separating loops are detected. The surface is then cut by adding two boundaries. The cutting process reduces the genus by one. The algorithm is run until the genus is null.

To reduce the shape complexity of the brain due to its multiple folding nature, meshes need to be inflated. Several methods have been developed in the literature to unfold the meshes[11]. The approach we adopted is based on CARET[12]. The position of each vertex is updated iteratively as a weighted sum of its current position and of the mean position of the neighbouring vertices. The sulcal depth is the geodesic distance covered by each point between its original and final locations. It corresponds to the local geometry information that has been lost during the inflation process and it is used as a local descriptor of the mesh shape later in the pipeline to help the shape matching.

Non-rigid registration of all individual meshes to a common template is performed with a shape context based algorithm as in [13]. Shape context is a compact, highly discriminative shape descriptor. For each point, a histogram of the relative polar coordinate of the other points of the mesh is constructed. However the method is time consuming and to reduce the processing time, the template and the floating meshes are decimated respectively to 3,000 and 2,000 points. The cost of matching a vertex  $m_i$  of the moving mesh to the vertex  $f_j$  of the template mesh is given by:

$$C_{i,j} = \frac{1}{2} \sum_{k=1}^K \frac{|h_i(k) - g_j(k)|^2}{h_i(k) + g_j(k)}$$

Where  $h_i$  and  $g_j$  are respectively the shape context histograms of points  $m_i$  and  $f_j$ . The best match between both meshes is obtained by finding the minimum path in the cost matrix  $C_{ij}$  with the Hungarian algorithm. The deformation vector field is calculated and propagated to the full mesh with an algorithm using the thin plate spline. In a second iteration of the shape context registration, local geometrical mesh information is added by the used a sulcal depth cost function:

$$C_{i,j}^{SD} = \frac{s_j - r_j}{N}$$

where  $s_j$  and  $r_j$  are respectively the sulcal depth of points  $m_i$  and  $f_j$ .

Cortical thickness values are propagated from the image to the registered mesh and are then smoothing with a Gaussian kernel at 5mm. At the end of the pipeline, each vertex of the mesh template is then associated to a cortical thickness vector corresponding to the thickness values of all patients at the same location point. Statistical analysis can then be processed between the different groups at each vertex location. Binaries for segmentation, cortical thickness estimation, Surface topological correction and registration are available as part of MILXView at our CSIRO software website<sup>1</sup>.

## 2.2 Group comparison

In the PiB- HC group, linear regressions are calculated at each vertex to remove the effect of age and years of education in the cortical thickness estimation. Parameters of the regressions are saved in order to process subjects in the other groups with the same regression. This correction removes the natural effect of age and year of education on all the groups. A vertex-wise T-test is then performed between the PiB- HC and the AD group. The significant level threshold is set to 0.001 to only capture the most significant regions. The p-values of the statistical tests are FDR corrected.

All individual AAL segmentations are propagated from the image to the common template. A multiple label STAPLE algorithm generates an AAL consensus segmentation. Significant regions are then intersected with the AAL mask to generate the significant part of each AAL region. Small size regions are removed. All individual mean cortical thicknesses are calculated in the significant patch of each anatomical region. Three different T-tests are performed, while controlling for the age and years of education in each tessellated region between AD, PiB- and PiB+ HC.

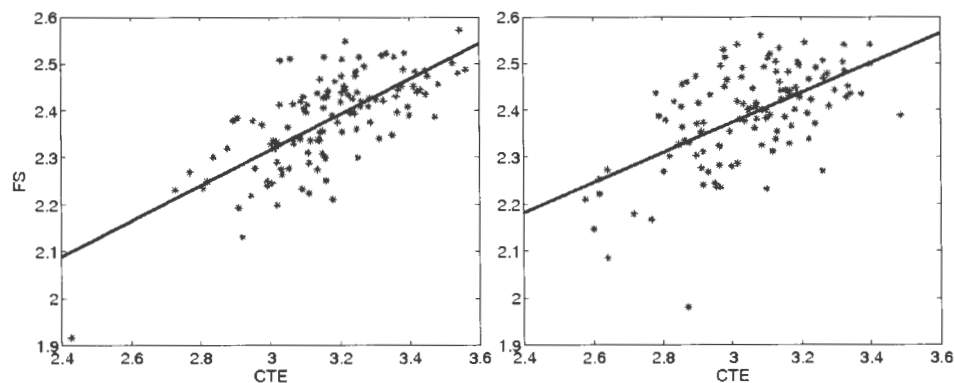


Figure 1: Comparison between our cortical thickness estimation (CTE) and FS one in the middle temporal lobe.

<sup>1</sup> <http://www.milxview.csiro.au>

### 3. RESULTS

In a first experiment we compared our results with FreeSurfer (FS) software [3]. Figure 1 presents the correlation between cortical thickness estimations using FreeSurfer and our approach (CTE) and in the middle temporal lobe in the left and right hemispheres. The corresponding correlations are around 0.7 and 0.58. Similar results were obtained in other AAL regions. The cortical estimation appears larger with CTE than FS. This difference can be due to the different initialisation of the cortical estimation.



Figure 2: T-test of the cortical thickness corrected by age and years of education and smoothed at 5mm between PiB- HC subjects and AD patients at level of significant (in red). Statistics are FDR corrected.

Figure 2 shows the one-tailed T-Test on the corrected cortical thickness values between AD and PiB- HC. Cortical atrophy for AD is highly significant principally in the temporal lobe, in the hippocampus region and in the precuneus.



Figure 3: The AAL Surface templates

T-tests between the three different groups have been processed in each significant part of each AAL region (Figure 3). Only major AAL regions with a p-value for the T-test between PiB+ HC and PiB- HC lower than 0.05 are reported in Table 1. They are also mapped on the template with p-values mapped as scalars on Figure 3. In Table 1, T-test between PiB- HC and AD is very significant for all regions. The tests between PiB+ HC and AD are all significant but with higher p-values.



Figure 4: The significant regions of the T-test on the corrected cortical thickness smooth at 5mm between the PiB- and PiB+ HC with the significant P-values as scalars.

The PiB+ HC group hence appears closer to the AD group than the PiB- HC is. We also observed a hemisphere asymmetry, more AAL regions appears significant on the left hemisphere than on the right one. The cortical thickness reduction in PiB+ HC is significant in some regions of the Frontal lobe, in the Hippocampus region, the occipital lobe (Calcarine fissure, Cuneus, Lingual gyrus, Inferior occipital gyrus) and in the temporal lobe and pole. While on the right hemisphere, only the medial and paracingulate gyri, the hippocampus and the temporal lobe are significant. The presence of  $\beta$ -amyloid plaques appears to act early in the degeneration of the cortex and to affect earlier the left hemisphere.

Figure 4 shows the real and Gaussian model distributions of the three groups in the Hippocampus region on the left hemisphere. The distribution of the PiB+ HC is in-between the two other distributions. The two histogram graphics show a larger difference between PiB+ and PiB- HC with the cortical thickness estimation couple with a surface based method than the hippocampus volume voxel based estimation.

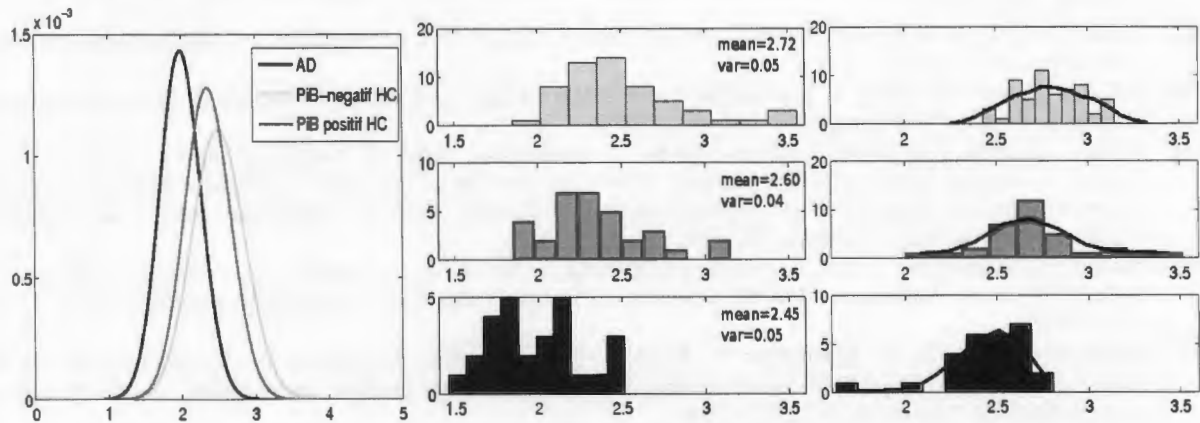


Figure 5: The graphic on the left side represents the Gaussian model distribution of the mean cortical thickness in the significant region of the Hippocampus for the three different groups. The graphic in the middle represents the histogram of the real values in the whole region, while the graphic on the right presents the cortical thickness histogram in the significant region of the right Hippocampus and its density curve fitting.

#### 4. CONCLUSION

In this paper, we presented a new surface based approach to perform cortical thickness comparison between AD prodromal groups and healthy elder subjects. This new pipeline makes it possible to unveil some significant cortical thickness difference between PiB+ and PiB-HC in regions of high cortical atrophy in AD patients. Compare to Freesurfer the new pipeline is fast (less than 2 hours for each subject).

AAL regions left hemisphere	p-values of the different T-tests		
	HC PiB-/AD	HC PiB+/AD	HC PiB-/HC PiB+
Middle Frontal gyrus	5.8508e-09	1.1885e-04	5.4494e-03
Median cingulate and paracingulate gyri	4.2212e-08	3.0259e-04	4.4863e-02
Hippocampus	1.9488e-09	6.7518e-06	2.3796e-02
ParaHippocampal gyrus	9.5609e-15	1.6917e-08	4.1370e-02
Middle occipital gyrus	4.8308e-08	1.0969e-03	1.4404e-02
Postcentral gyrus	9.1999e-12	2.0708e-06	2.1342e-02
SupraMarginal gyrus	1.2867e-11	2.2551e-04	3.7527e-03
Precuneus	4.7868e-14	1.7414e-05	5.4458e-04
Superior temporal gyrus	3.4842e-14	2.1653e-05	3.2545e-03
Middle temporal gyrus	2.1745e-15	6.9104e-07	9.6079e-03
right hemisphere	HC PiB -/AD	HC PiB +/AD	HC PiB-/HC PiB+
Median cingulate and paracingulate gyri	3.3122e-05	1.2262e-02	2.4115e-02
Hippocampus	1.4080e-11	1.4470e-04	2.4624e-02
Middle temporal gyrus	2.4929e-08	5.3737e-03	7.7670e-04
Inferior temporal gyrus	1.5580e-07	5.3372e-04	1.1656 e-02

Table 1: The table reports the P-values of the T-Tests on the mean individual cortical thickness (smoothed at 5 mm) between PiB+, PiB- HC and AD.



## REFERENCES

- [1] Ziolkowski, S., Weissfeld, L., Klunk, W., Mathis, C., Hoge, J., Lopresti, B., DeKosky, S., Price, J.: Evaluation of voxel-based methods for the statistical analysis of PIB PET amyloid imaging studies in Alzheimer's disease. *Neuroimage* 33(1), 94–102 (2006)
- [2] Dale, A., Fischl, B., Sereno, M.: Cortical Surface-Based Analysis\* 1: I. Segmentation and Surface Reconstruction. *Neuroimage* 9(2), 179–194 (1999)
- [3] Fischl, B., Sereno, M., Dale, A.: Cortical Surface-Based Analysis\* 1: II: Inflation, Flattening, and a Surface-Based Coordinate System. *Neuroimage* 9(2), 195–207 (1999)
- [4] Kathryn A. Ellis, Christopher C. Rowe, Victor L. Villemagne, Ralph N. Martins, Colin L. Masters, Olivier Salvado, Cassandra Szoek, and David Ames. Addressing population aging and Alzheimer's disease through the Australian Imaging Biomarkers and Lifestyle study: Collaboration with the Alzheimer's disease Neuroimaging Initiative. *Alzheimer's and Dementia*, 6(3):291-296, May 2010
- [5] Raniga, P., Bourgeat, P., Fripp, J., Acosta, O., Villemagne, V., Rowe, C., Masters, C., Jones, G., O'Keefe, G., Salvado, O., et al.: Automated 11C-PiB Standardized Uptake Value Ratio. *Academic radiology* 15(11), 1376–1389 (2008)
- [6] Bourgeat, P., Chételat, G., Villemagne, V., Fripp, J., Raniga, P., Pike, K., Acosta, O., Szoek, C., Ourselin, S., Ames, D., et al.:  $\beta$ -Amyloid burden in the temporal neocortex is related to hippocampal atrophy in elderly subjects without dementia. *Neurology* 74(2), 121 (2010)
- [7] Tzourio-Mazoyer, N., Landeau, B., Papathanassiou, D., Crivello, F., Etard, O., Delcroix, N., Mazoyer, B., Joliot, M.: Automated anatomical labeling of activations in SPM using a macroscopic anatomical parcellation of the MNI MRI single-subject brain. *Neuroimage* 15(1), 273–289 (2002)
- [8] Rueda, A., Acosta, O., Bourgeat, P., Fripp, J., Bonner, E., Dowson, N., Couprie, M., Romero, E., Salvado, O.: Partial volume estimation of brain cortex from MRI using topology-corrected segmentation. In: *Biomedical Imaging: From Nano to Macro, 2009. ISBI'09. IEEE International Symposium on*. pp. 133–136. IEEE (2009)
- [9] Acosta, O., Bourgeat, P., Zuluaga, M., Fripp, J., Salvado, O., Ourselin, S.: Automated voxel-based 3D cortical thickness measurement in a combined Lagrangian-Eulerian PDE approach using partial volume maps. *Medical Image Analysis* 13(5), 730–743 (2009)
- [10] Favreau, J., Hemm, S., Nuti, C., Coste, J., Barra, V., Lemaire, J.: A tool for topographic analysis of electrode contacts in human cortical stimulation. In: *Computer Vision, 2007. ICCV 2007. IEEE 11th International Conference on*. pp. 1–6. IEEE (2007)
- [11] Tosun, D., Rettmann, M., Han, X., Tao, X., Xu, C., Resnick, S., Pham, D., Prince, J.: Cortical surface segmentation and mapping. *NeuroImage* 23, S108–S118 (2004)
- [12] Bonner, E., Acosta, O., Fripp, J., Salvado, O.: A quantitative comparison of three methods for inflating cortical meshes. In: *2009 IEEE International Symposium on Biomedical Imaging: From Nano to Macro*. pp. 1338–1341. IEEE (June 2009)
- [13] Acosta, O., Fripp, J., Rueda, A., Xiao, D., Bonner, E., Bourgeat, P., Salvado, O.: 3D shape context surface registration for cortical mapping. In: *2010 IEEE International Symposium on Biomedical Imaging: From Nano to Macro*. pp. 1021–1024. IEEE, Rotterdam, The Netherlands (14–17 April 2010)